Structures and Energetics of Hydrated Oxygen Anion Clusters

Daniel M. Chipman* and John Bentley

Radiation Laboratory, University of Notre Dame, Notre Dame, Indiana 46556

Received: May 11, 2005; In Final Form: June 20, 2005

Hydration of the atomic oxygen radical anion is studied with computational electronic structure methods, considering $(O^-)(H_2O)_n$ clusters and related proton-transferred $(OH^-)(OH)(H_2O)_{n-1}$ clusters having $n = 1-5$. A total of 67 distinct local-minimum structures having various interesting hydrogen bonding motifs are obtained and analyzed. On the basis of the most stable form of each type, $(O^-)(H_2O)_n$ clusters are energetically favored, although for $n \geq 3$, there is considerable overlap in energy between other members of the $(O^-)(H_2O)_n$ family and various members of the $(OH^-)(OH)(H_2O)_{n-1}$ family. In the lower-energy $(O^-)(H_2O)_n$ clusters, the hydrogen bonding arrangement about the oxygen anion center tends to be planar, leaving the oxygen anion p-like orbital containing the unpaired electron uninvolved in hydrogen bonding with any water molecule. In $(OH^-)(OH)(H_2O)_{n-1}$ clusters, on the other hand, nonplanar arrangements are the rule about the anionic oxygen center that accepts hydrogen bonds. No instances are found of OH^- acting as a hydrogen bond donor. Those OH bonds that form hydrogen bonds to an anionic O^- or OH^- center are significantly stretched from their equilibrium value in isolated water or hydroxyl. A quantitative inverse correlation is established for all hydrogen bonds between the amount of the OH bond stretch and the distance to the other oxygen involved in the hydrogen bond.

Introduction

Atomic oxygen radical anion, O^-, is an important component of irradiated basic aqueous solutions.[1] The nucleophilic O^- undergoes aqueous reactions that are somewhat different from those of its conjugate base, the electrophilic and weakly acidic hydroxyl radical, OH ($pK_a \approx 12$).[2,3] For example, O^- readily combines with O_2 (forming O_3^-), whereas OH does not.[4] Many rate constants for various aqueous reactions of O^- have been reported,[5] and its general chemistry has been reviewed.[6] An aqueous radiolytic study[7] has also investigated the relative probabilities of proton transfer vs hydrogen atom transfer in the $O^- + H_2O \rightarrow OH^- + OH$ reaction.

While it can be expected that O^- forms strong hydrogen bonds to solvent water molecules, very little is known about the actual structure of O^- and its environs in aqueous solution. In this connection, it is of interest to note that electron spin resonance (ESR) observation of O^- in equilibrium with OH in irradiated ice was interpreted[8] to indicate that hydrogen bonds to water are formed in the plane of the two doubly occupied p-orbitals of O^-, but no hydrogen bonds are formed with the singly occupied p-orbital.

The study of gas-phase hydrated clusters is an effective means to help understand solvation effects in the condensed phase. Indeed, the structure and energetics of the gas-phase hydrate clusters (for which we use the generic designation of $O_{n+1}H_{2n}^-$ to indicate O^- complexed with n water molecules in order to avoid any specific structural implications) have been of considerable experimental interest since the early detection by mass spectrometry of the monohydrate $O_2H_2^-$ in a $H_2/O_2/N_2$ flame.[9] The monohydrate complex of presumed structure $(O^-)(H_2O)$, in which H_2O forms one strong hydrogen bond to O^-, was postulated[10] as a long-lived intermediate in order to explain the kinetics of the reaction $O^- + H_2O \rightarrow OH^- + OH$ studied by mass spectrometry. Analysis of flowing afterglow experiments on the association of O^- with H_2O in the presence of various third bodies led to the suggestion[11] that the putative species $(O^-)(H_2O)$ may be better described as $(OH^-)(OH)$, in which the OH radical forms a strong hydrogen bond to OH^-. In a study of the reaction $O^- + H_2O \rightarrow OH^- + OH$ carried out in an ion-beam collision chamber with different oxygen isotopes, it was suggested[12] that both $(O^-)(H_2O)$ and $(OH^-)(OH)$ may be distinct long-lived species, with the former being more stable than the latter. This idea of two distinct monohydrate species was also considered, but without definite conclusion, in several later experimental investigations.[13−17] Mass spectrometric study[18] of $O_{n+1}H_{2n}^-$ clusters with $n = 0-59$ has indicated especially stable structures with "magic numbers" of $n = 11$, 14, 17, and 20.

A number of previous theoretical studies have been carried out on the monohydrate of O^-. Early low-level ab initio calculations[19−21] reported a high-energy species $(HO\therefore OH)^-$, in which two equivalent OH moieties joined by a long 2-center−3-electron OO bond share the extra electron equally. Later ab initio calculations[22,23] have established that the true equilibrium structure corresponds instead to planar $(O^-)(H_2O)$ with a single nearly linear hydrogen bond between O^- and H_2O. Subsequent ab initio studies have explored the potential surface for interconnection between the $(HO\therefore OH)^-$ and $(O^-)(H_2O)$ structures.[24−26] A comprehensive study[27] at various levels of ab initio theory, pure DFT (i.e., density functional theory without including any exact exchange), and hybrid DFT reported that in addition to the most stable $(O^-)(H_2O)$ structure there is indeed also a local-minimum nonplanar $(HO\therefore OH)^-$ form with C_2 symmetry. Pure DFT methods erroneously indicate the latter to be the global minimum, while ab initio and hybrid DFT methods consistently show it to be significantly higher in energy

10.1021/jp052472b CCC: $30.25
Published on Web 07/30/2005

than $(O^-)(H_2O)$. Studies of a possible structure having a proton-transferred $(OH^-)(OH)$ form[16,17,25] have found it be of only slightly higher energy than $(O^-)(H_2O)$, but no unambiguous characterization has been given of $(OH^-)(OH)$ as a true local minimum on the potential surface. An ab initio study[28] has further reported very high energy $(HOO^-)(H)$ and $(O_2^-)(H_2)$ structures.

Several theoretical works have also reported equilibrium structures for various larger hydrate clusters. Calculations[29] using pure DFT on clusters with $n = 1-3$ found that the lowest-energy structures correspond to $(OH^-)(OH)(H_2O)_{n-1}$. A later study up to $n = 6$ using ab initio methods[30] found that for $n = 2-4$ the most stable structure corresponds to $(OH^-)(OH)(H_2O)_{n-1}$, while for $n = 5-6$ (which were done at a lower level of theory), the additional water molecules start to form a second solvation shell and instead have $(O^-)(H_2O)_n$ as their most stable structures. A subsequent work[31] estimated the $H\cdots O^-$ hydrogen bonding distance for $(O^-)(H_2O)_n$ clusters in the thermodynamic limit of large n. In a study using hybrid DFT methods up to $n = 4$, we have considered[32] planar symmetrical structures of the form $(O^-)(H_2O)_n$. Another study[33] up to $n = 4$ also using hybrid DFT methods considered a few representative structures of both the $(O^-)(H_2O)_n$ and $(OH^-)(OH)(H_2O)_{n-1}$ forms, finding (in marked contrast to the above-discussed ab initio study[30]) that the $(O^-)(H_2O)_n$ form consistently provided the most stable structures.

Let us summarize here this brief survey on structural evidence to date. For very large values of n, the experimental pK_a of OH in bulk water clearly indicates that the $(O^-)(H_2O)_n$ form is more stable than $(OH^-)(OH)(H_2O)_{n-1}$. The scant experimental evidence on small clusters is inconclusive for structural questions. The computational evidence for the $n = 1$ case clearly shows $(O^-)(H_2O)$ to be the most stable form, suggests that the proton-transferred $(OH^-)(OH)$ structure is only slightly higher in energy but may not be a true local minimum on the potential surface, and also indicates the presence of several other high-energy local-minimum structures. For other small values of $n \geq 2$, the computational evidence is mixed, such that there still remains ambiguity about the relative stability of $(O^-)(H_2O)_n$ versus $(OH^-)(OH)(H_2O)_{n-1}$ structures.

The present work reports calculations on the $n = 1-5$ clusters. One purpose is to apply higher levels of theory together with a thorough search among possible structures having both $(O^-)(H_2O)_n$ and $(OH^-)(OH)(H_2O)_{n-1}$ motifs to help resolve these structural questions. We find and report a total of 67 local-minimum structures, which include almost all of the structures previously described in the literature and many more besides. None of the work on $O_{n+1}H_{2n}^-$ to date has examined the vibration frequencies of the clusters, and another purpose is to provide a foundation for further calculations aimed at interpreting recent experimental observations[34] on the infrared spectra of these clusters.

Computational Methods

To balance economy with accuracy, we chose for geometry optimizations the B3LYP method[35,36] together with the 6-31+G(d) basis set.[37-39] Such a hybrid DFT method avoids the problems with pure DFT documented by Hrusak et al.[27] Local minima were confirmed by the absence of imaginary frequencies in the B3LYP/6-31+G(d) harmonic vibrational analysis. The zero-point vibrational energy (ZPVE) was obtained from the sum of harmonic frequencies, which for this purpose were multiplied by the recommended[40] scaling factor of 0.9806.

For better electronic energies, single-point calculations at the optimum B3LYP/6-31+G(d) geometries were carried out using the MP4(SDQ) method[41,42] together with the 6-311+G(2d,p) basis set.[43,44] The resulting MP4(SDQ)/6-311+G(2d,p)//B3LYP/6-31+G(d) energies were corrected for basis set superposition error (BSSE) using the full counterpoise correction.[45] To check the reliability of the B3LYP/6-31+G(d) structures, geometry optimizations were also carried out at the MP4(SDQ)/6-311+G-(2d,p) level on several representative small clusters; for brevity, the double slash notation is not used where the same method was used for both energy and geometry determination. Some calculations were also done with various basis sets to evaluate the reliability of the MP2 method[41] for these clusters.

As a check, the high-level QCISD(T) method[46] was also used on some of the smallest clusters for single-point energy evaluation at the corresponding QCISD geometry, together with the aug-cc-pVTZ basis set[47,48] for each.

All of the radicals examined in this work are doublet states. We examined the quantity $\langle S^2 \rangle$, the expectation value of the square of the electronic spin operator, and found it to be between 0.75 and 0.76 for all radicals studied. This indicates that spin contamination by quartet or higher states poses no significant problem for the results presented here.

Computation of equilibrium geometries, energies, and harmonic frequencies was carried out with the *Gaussian 98*[49] and *Gaussian 03*[50] programs.

Because our results may be compared with experimental data collected from systems that are not necessarily in thermodynamic equilibrium, we want to identify as many low-lying structures as possible. Different starting points for geometry optimizations were generated from a number of sources. These included our previous work[32] on $(O^-)(H_2O)_n$ and the various $(O^-)(H_2O)_n$ and $(OH^-)(OH)(H_2O)_{n-1}$ structures reported by Knak Jensen.[30] In addition, $(OH^-)(H_2O)_n$ structures[51,52] with OH^- replaced by O^- as well as $(H_2O)_n$ structures[53] with one of the waters replaced by O^- were also considered. Further structures were identified by modifying previously identified structures and by adding additional waters to known small clusters.

Notation

We employ a notation to describe the isomers of $O_{n+1}H_{2n}^-$ which reflects the hydrogen bond networks within the clusters. Since the anionic center is primarily responsible for driving the hydrogen bonding patterns in these clusters, the notation reflects the solvation shell structure of the anion. The general form is $A_aB_bC_c...$, in which $n = A + B + C + ...$ with A being the number of molecules (either water or hydroxyl) in the first solvation shell about the anion, B the number in the second shell (if any), and so forth. The subscripts represent the number of hydrogen bonds for which molecules of that shell act as acceptors, so that $A + a + b + c + ...$ is the total number of hydrogen bonds in the cluster. With the $(OH^-)(OH)(H_2O)_{n-1}$ families, an asterisk is used to indicate in which shell the hydroxyl radical resides.

For instance, 2_21_0 indicates a cluster having two water molecules in the first solvation shell, each forming a hydrogen bond to O^-, and one water in the second solvation shell that donates a hydrogen bond to each of the first-shell waters. As another example, $2^*_21_0$ refers to a cluster in which a water molecule and a hydroxyl radical in the first shell each donate a hydrogen bond to OH^-, and a water in the second shell donates a hydrogen bond to the first water and to the hydroxyl. If more than one cluster have the same designation in this notation, they are distinguished by appending an additional parenthetical label

TABLE 1: Calculated MP4(SDQ)/6-311+G(2d,p)//B3LYP/6-31+G(d) Binding Energies in kcal/mol of Various $O_{n+1}H_{2n}^-$ Clusters

	elec	BSSE	elec + BSSE	ΔZPVE	$\Delta E°_0$		elec	BSSE	elec + BSSE	ΔZPVE	$\Delta E°_0$
					$n = 1$: $(O^-)(H_2O)$						
1_0	−25.8	2.1	−23.6	0.0	−23.6						
					$n = 2$: $(O^-)(H_2O)_2$						
2_0(a)	−46.2	3.6	−42.6	2.5	−40.1	2_0(b)	−46.1	3.6	−42.5	2.5	−40.0
					$n = 2$: $(OH^-)(OH)(H_2O)$						
$2*_0$	−45.5	5.0	−40.5	1.0	−39.5						
					$n = 3$: $(O^-)(H_2O)_3$						
3_0	−64.4	5.5	−58.9	4.4	−54.5	2_21_0(a)	−62.8	6.2	−56.7	5.5	−51.2
3_1	−63.6	5.4	−58.2	5.0	−53.2	2_11_0	−60.4	5.5	−54.9	4.6	−50.3
2_21_0(b)	−62.7	5.8	−56.9	5.4	−51.4						
					$n = 3$: $(OH^-)(OH)(H_2O)_2$						
$3*_0$	−62.9	6.4	−56.5	3.8	−52.7	$2*_21_0$(b)	−61.6	6.9	−54.6	3.9	−50.7
$3*_1$	−63.9	6.9	−57.0	4.4	−52.6	$2*_11_0$(b)	−59.4	6.9	−52.5	2.8	−49.7
$2*_21_0$(a)	−62.0	6.9	−55.2	4.1	−51.1	$2*_11_0$(a)	−59.6	6.9	−52.7	3.1	−49.6
					$n = 4$: $(O^-)(H_2O)_4$						
4_2(a)	−78.9	6.9	−71.9	7.8	−64.1	3_21_0(d)	−76.2	7.1	−69.1	7.3	−61.9
4_2(b)	−78.4	6.5	−71.9	7.9	−64.0	3_21_0(e)	−76.1	7.2	−69.0	7.1	−61.8
3_21_0(b)	−79.3	7.8	−71.5	7.8	−63.8	4_4	−78.3	8.0	−70.3	9.3	−61.0
3_21_0(a)	−79.3	7.7	−71.6	7.8	−63.8	3_21_1(a)	−78.4	8.4	−70.0	9.1	−61.0
3_21_0(c)	−76.6	7.2	−69.4	7.2	−62.2	3_21_1(b)	−78.0	8.3	−69.7	9.0	−60.7
3_11_1	−77.3	7.8	−69.5	7.4	−62.1	2_22_1	−74.3	8.3	−66.0	7.7	−58.3
					$n = 4$: $(OH^-)(OH)(H_2O)_3$						
$3*_21_0$(a)	−79.8	8.9	−70.9	7.6	−63.3	$3*_11_0$	−75.6	8.2	−67.4	6.0	−61.5
$4*_1$	−78.9	9.1	−69.8	7.2	−62.6	$3*_21_0$(e)	−77.6	9.0	−68.6	7.2	−61.3
$3*_21_0$(c)	−77.9	8.5	−69.4	6.9	−62.5	$3*_11_1$	−76.8	9.0	−67.9	7.1	−60.8
$3*_21_1$(a)	−79.8	9.2	−70.5	8.1	−62.5	3_11*_1(a)	−75.5	8.9	−66.6	6.1	−60.5
$3*_21_0$(d)	−77.7	8.5	−69.2	6.8	−62.4	3_11*_0	−74.8	8.8	−66.0	6.0	−60.0
$3*_21_0$(b)	−78.7	8.9	−69.8	7.6	−62.2	3_11*_1(b)	−74.3	9.1	−65.2	5.7	−59.5
$3*_21_1$(b)	−78.4	9.1	−69.3	7.7	−61.6	$2*_21_11_0$	−74.2	8.8	−65.4	6.1	−59.3
					$n = 5$: $(O^-)(H_2O)_5$						
4_31_0(a)	−92.9	9.0	−83.8	10.7	−73.2	3_22_1	−90.7	9.6	−81.1	9.9	−71.1
3_42_0	−93.4	9.8	−83.7	11.2	−72.4	4_41_1(b)	−92.9	10.0	−83.0	12.3	−70.6
4_41_1(a)	−93.9	8.7	−85.1	13.0	−72.1	3_32_2(a)	−93.0	10.5	−82.5	12.1	−70.4
$3_21_11_0$	−91.2	9.5	−81.7	10.0	−71.7	3_32_2(b)	−90.0	11.1	−78.9	12.5	−66.4
4_31_0(b)	−90.0	8.5	−81.5	10.2	−71.3	$2_22_31_0$	−86.5	10.2	−76.3	9.9	−66.4
5_5	−91.7	9.4	−82.3	11.1	−71.2						
					$n = 5$: $(OH^-)(OH)(H_2O)_4$						
$3*_32_2$(a)	−94.3	10.9	−83.4	11.3	−72.1	$3*_32_1$	−90.6	11.1	−79.6	9.5	−70.1
3_32*_0	−91.5	10.7	−80.8	9.2	−71.6	$3*_32_2$(b)	−91.5	11.7	−79.8	11.1	−68.7
$3*_32_2$(c)	−94.2	11.4	−82.8	11.3	−71.5	3_22*_1	−88.8	10.9	−77.9	9.5	−68.3
$3*_21_11_0$	−91.7	10.7	−81.0	9.8	−71.2	$3*_22_2$(a)	−89.7	11.2	−78.6	10.6	−68.0
$3*_42_0$	−91.7	10.7	−81.0	10.0	−70.9	$2*_32_11_1$	−88.3	11.3	−77.1	9.3	−67.8
$4*_31_0$	−92.4	11.1	−81.3	10.4	−70.9	3_22*_2	−87.3	11.0	−76.3	9.7	−66.6
4_31*_1	−91.7	10.4	−81.4	10.6	−70.8	$3*_22_2$(b)	−88.4	11.6	−76.8	10.9	−65.9
$4*_41_1$	−94.4	12.0	−82.4	11.8	−70.6						

of (a), (b), (c), and so forth; such clusters usually have the same general structure, differing only in the orientation of dangling OH bonds.

Energetics

The total energy $E°_0$ at 0 K of each structure is obtained by adding the single-point electronic energy including nuclear repulsion (elec), the BSSE correction, and the ZPVE. In Table 1, we report binding energies $\Delta E°_0$ corresponding to the process

$$O^- + nH_2O \rightarrow O_{n+1}H_{2n}^- \quad (1)$$

for 67 minimum-energy configurations of $O_{n+1}H_{2n}^-$ involving $n = 1-5$.

For $n = 1$ and 2, we are confident that there are no other low-lying equilibrium structures (within the computational methods we used). For $n \geq 3$, we cannot state that we have found all possible structures; this task would be prohibitive for $n = 4$ and 5 anyway. However, we feel that we have found the important lowest-energy structures, or at least that any additional low-lying structure will be closely related to one of the structures reported here by simple reorientation of a non-hydrogen-bound ("dangling") OH bond and so will otherwise have very nearly the same structure and energy.

The BSSE correction decreases the binding energy of a complex by removing an artificial source of stabilization. BSSE increases with the size of the cluster because each additional constituent makes additional orbitals available to lower the energies of the other constituents. This is clearly seen in Table 1: for the sequence of all $O^-(H_2O)_n$, the average BSSE values for $n = 1-5$ are 2.1, 3.6, 5.7, 7.6, and 9.7 kcal/mol. A similar trend is exhibited by the sequence of all $(OH^-)(OH)(H_2O)_{n-1}$.

A more interesting effect is the differential influence of BSSE on $O^-(H_2O)_n$ versus $(OH^-)(OH)(H_2O)_{n-1}$ structures. Comparing analogous structures, the latter are destabilized by at least 1.1 kcal/mol relative to the former for all n. This places the lowest-energy structure of $O^-(H_2O)_n$ below that of $(OH^-)(OH)(H_2O)_{n-1}$ for all n studied, whereas uncorrected electronic energies would

put $(OH^-)(OH)(H_2O)_{n-1}$ lower for $n = 4$ and 5. Finally, the BSSE correction produces some changes in order of stability within the separate $O^-(H_2O)_n$ and $(OH^-)(OH)(H_2O)_{n-1}$ structural families. Structures which benefit from this (i.e., have the smallest BSSE) are typically those with relatively fewer hydrogen bonds between water molecules.

The column marked ΔZPVE in Table 1 denotes the binding energy contribution arising from the change in ZPVE between an $O_{n+1}H_{2n}^-$ complex and n free water molecules. Each additional water molecule in a complex therefore adds the contributions of six new intermolecular vibrational modes to ΔZPVE.

As with the BSSE correction, inclusion of ΔZPVE also decreases the binding energy of a complex. For a given n, inclusion of ΔZPVE generally favors $(OH^-)(OH)(H_2O)_{n-1}$ over analogous $O^-(H_2O)_n$ structures, but the effect is somewhat less than the BSSE effect so that structures of the $O^-(H_2O)_n$ form remain lowest in energy for all n considered. Within a family of either $O^-(H_2O)_n$ or $(OH^-)(OH)(H_2O)_{n-1}$ structures, inclusion of ΔZPVE sometimes has a substantial effect on the binding energy ordering. Structures which are most stabilized (i.e., have the smallest ΔZPVE) are generally those with the lowest total number of hydrogen bonds.

Our goal in this work is limited to characterizing ground states of the clusters. However, some excited states were unavoidably encountered during the course of the calculations. These were always found to lie about 1 kcal/mol or more above the respective ground states and, except for the case of $n = 1$, are not discussed any further in this work.

$O_2H_2^-$ Structures. This species has been previously studied by a variety of computational methods. Of particular value is the work of Hrusak et al.,[27] who summarized the prior studies and provided a direct comparison of the results from more than a dozen computational methods. Hybrid DFT methods and ab initio methods all consistently led to a minimum-energy structure of the $(O^-)(H_2O)$ form, with charge and spin highly localized on the ionic oxygen atom and with a strong nearly linear hydrogen bond between O^- and water. Pure DFT methods incorrectly found the global-minimum structure to be $(HO\therefore OH)^-$, whereas in fact, this form does not even merit our serious attention because at high levels of ab initio theory Hrusak et al. found it to be of high energy. For example, at the sophisticated CCSD(T)/POL+df level, the electronic energy of $(HO\therefore OH)^-$ was found to lie 10.3 kcal/mol above that of the global-minimum $(O^-)(H_2O)$ form. On the other hand, $(OH^-)(OH)$, which has been treated by several workers, although not by Hrusak et al., must be considered as a serious low-energy candidate. But despite considerable speculation about the possibility of a local-minimum $(OH^-)(OH)$ structure, only one reported calculation[17] has actually found it, and that at the complete active space self-consistent field (CASSCF) level of theory which neglects most dynamical electron correlation and so should not be regarded as definitive.

The minimum-energy structure 1_0 for $(O^-)(H_2O)$ is planar, as shown in Figure 1. There are three possible orientations for the oxygen 2p orbital containing the unpaired electron: perpendicular to the molecular plane (π_{out}), perpendicular to the hydrogen bond but in the molecular plane (π_{in}), or along the hydrogen bond (σ). The ground state corresponds to the $\sigma^2\pi_{in}^2\pi_{out}^1$ ($^2A''$) configuration. The lowest excited state has $\sigma^2\pi_{in}^1\pi_{out}^2$ ($^2A'$) configuration and lies 0.94 kcal/mol vertically above the ground state. The other possible $\sigma^1\pi_{in}^2\pi_{out}^2$ ($^2A'$) configuration is a high-lying excited state that we were not able to find as a bound structure. This can be rationalized in terms of the largely electrostatic character of the hydrogen bond that dictates a lower energy will be attained if the hydrogen approaches a doubly filled oxygen 2p orbital rather than a singly filled one that corresponds to a region of relative electron depletion.

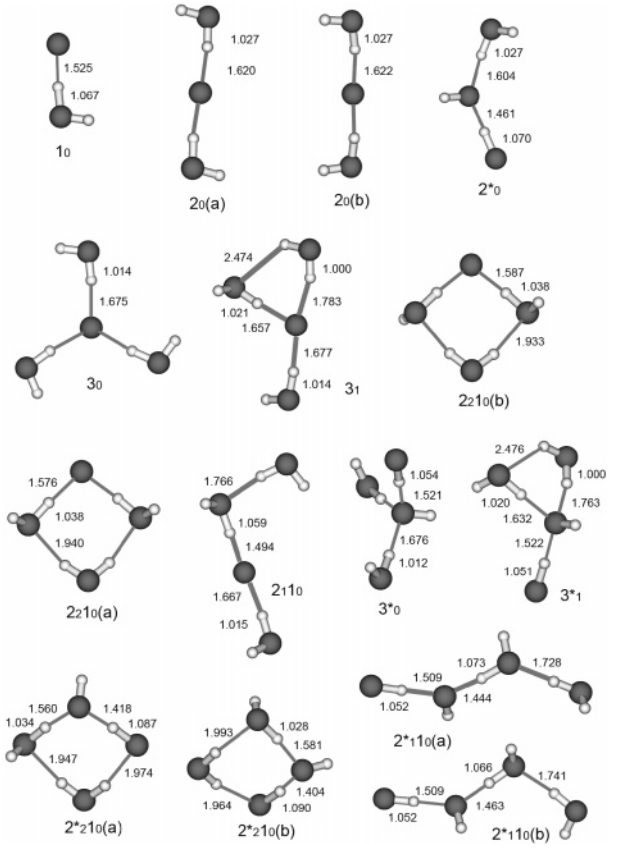

Figure 1. B3LYP/6-31+G(d) structures of $O_2H_2^-$, $O_3H_4^-$, and $O_4H_6^-$ clusters.

The equilibrium structures of $(O^-)(H_2O)$ obtained at various levels of theory are reported in Table 2. They are all in reasonably good agreement with one another and with the best previous results.[27] The largest discrepancies from the presumably accurate QCISD/aug-cc-pVTZ geometry lie in the hydrogen bond H···O, the bound OH, and the OO distances being too long by about 0.02, 0.02, and 0.03 Å, respectively, in the B3LYP/6-31+G(d) structure, and the H···O distance being about 0.02 Å too short in the MP4(SDQ)/6-311+G(2d,p) structure.

The putative 1^*_0 structure corresponding to $(OH^-)(OH)$ was not found to be a local minimum in our calculations. Attempts to optimize it at the B3LYP/6-31+G(d), MP4(SDQ)/6-311+G(2d,p), and QCISD/aug-cc-pVTZ levels of theory always led back to the 1_0 global minimum. Because of the extreme localization of the negative charge, description of the proton transfer in the smallest $n = 1$ cluster is more demanding in terms of electron correlation and basis set extension than in most of the larger clusters. This case therefore provides a challenging testing ground to evaluate the performance of various computational methods.

To study the tendency for proton transfer, we have determined the electronic energy versus the ΔR_{OH} coordinate that moves the central hydrogen nucleus in $(O^-)(H_2O)$ away from the water oxygen and toward the O^- center. For each given fixed value of ΔR_{OH}, constrained optimizations were carried out to relax all other geometrical parameters. The results are summarized in Figure 2, with symbols showing values calculated at 0.05 Å

TABLE 2: Structural Parameters Calculated for Planar (O^-)(H_2O), with Distances in angstroms and Angles in degrees[a]

method	$R_{H\cdots O}$	R_{OH}	R_{OH}	R_{OO}	θ_{HOH}	$\chi_{H\cdots OH}$
B3LYP/6-31+G(d)	1.490	1.075	0.969	2.562	102.4	174.5
MP4(SDQ)/6-311+G(2d,p)	1.453	1.067	0.961	2.519	102.4	176.3
QCISD(T)/aug-cc-pVTZ//QCISD/aug-cc-pVTZ	1.474	1.056	0.959	2.529	101.9	176.7

[a] The first column labeled R_{OH} refers to the hydrogen bonded OH of water and the second to the free OH of water.

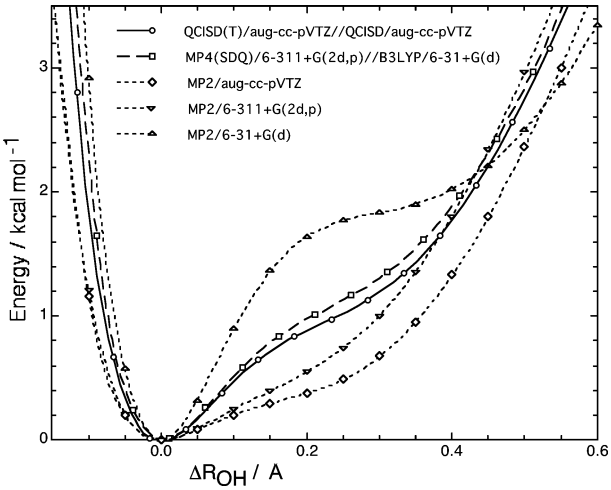

Figure 2. Electronic potential energy curves for stretching from equilibrium of the central hydrogen in (O^-)(H_2O), with full relaxation of all other geometrical parameters.

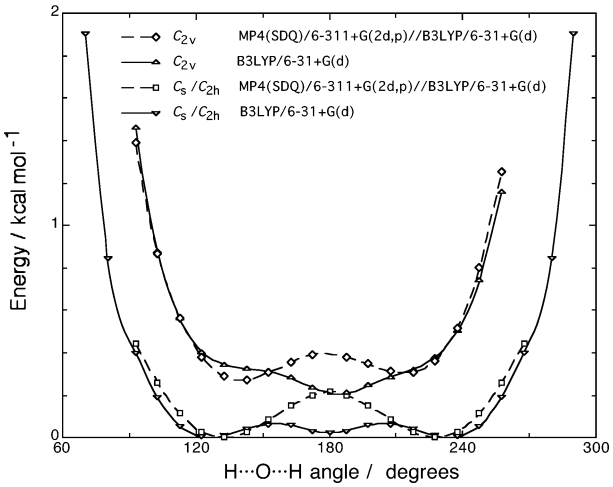

Figure 3. Electronic potential energy curves for H···O···H bending in (O^-)(H_2O)$_2$, with full relaxation of all other geometrical parameters.

increments of ΔR_{OH} joined by smooth lines obtained through spline interpolation. We regard the highest-level QCISD(T)/aug-cc-pVTZ//QCISD/aug-cc-pVTZ electronic energy curve as a reference that is likely to be highly accurate and compare results from other computational methods to it.

While there is no local minimum corresponding to (OH^-)(OH) at any of the levels of theory considered here, the QCISD(T)/aug-cc-pVTZ//QCISD/aug-cc-pVTZ curve in Figure 2 does show a pronounced shoulder at intermediate values of ΔR_{OH}. The CASSCF structure of (OH^-)(OH) reported in the literature[17] is very similar to those structures in Figure 2 found in the region of $\Delta R_{OH} = 0.40-0.45$ Å, which have QCISD(T)/aug-cc-pVTZ//QCISD/aug-cc-pVTZ electronic energies ranging from 1.8 to 2.2 kcal/mol above the minimum. The MP4(SDQ)/6-311+G(2d,p)//B3LYP/6-31+G(d) and MP4(SDQ)/6-311+G(2d,p) methods are quite accurate (the latter not being shown in the figure to avoid congestion), respectively lying only 0.1 and 0.2 kcal/mol higher in energy than the reference curve in this region. However, over the range of small to intermediate values of ΔR_{OH}, the MP2/6-31+G(d) method gives energies that are much too high, while the MP2/6-311+G(2d,p) and MP2/aug-cc-pVTZ methods each give energies that are much too low.

These observations lend support to the reasonableness of the MP4(SDQ)/6-311+G(2d,p)//B3LYP/6-31+G(d) method that, unless specifically noted otherwise, is used for the results reported in the rest of this paper. It also suggests that MP2 results found in the literature are suspect for evaluating the relative energies of proton-transferred versus nontransferred structures in these systems, regardless of the basis set used.

$O_3H_4^-$ Structures. The addition of a second water molecule opens up several possibilities for isomerization, as seen in Figure 1. The lowest-energy conformation is obtained by introducing the second water molecule near O^- on the side opposite the first water molecule, producing 2_0(a) which has a planar (O^-)(H_2O)$_2$ form. It is depicted in Figure 1 with a H···O···H angle of 180°, where its electronic state is $^2B_{3u}$ in C_{2h} symmetry.

However, 2_0(a) is quite fluxional. Figure 3 shows the electronic energy of 2_0(a) as the H···O···H angle is varied, with constrained optimizations to relax all other geometrical parameters. At angles away from 180°, the structure remains planar with electronic state $^2A''$ in C_s symmetry. At the B3LYP/6-31+G(d) level, the potential curve moving away from 180° first passes over a very small barrier and then falls into either of two equivalent local minima at an angle of 126°, or its complement of 234°, which lies 0.02 kcal/mol below the 180° structure. But with higher levels of theory, the local minimum at 180° disappears, becoming instead a transition state between the two equivalent C_s minima. As seen in Figure 3, with MP4(SDQ)/6-311+G(2d,p)//B3LYP/6-31+G(d) the C_s minima lie at a H···O···H angle of 133°, or its complement of 227°, and the C_{2h} transition state lies 0.21 kcal/mol higher. The B3LYP/6-311+G(2d,p) and MP4(SDQ)/6-311+G(2d,p) methods (not shown in the figure to avoid congestion) give very similar results, respectively placing the C_{2h} entity at 0.23 and 0.20 kcal/mol above the bent minima. The ZPVE can easily overcome such shallow electronic energy barriers and allow facile visitation of a wide range of H···O···H angles. We conclude that 2_0(a) can be regarded as being linear on average, but with a very flat potential surface[54] that allows for many readily accessible bent conformations as well.

Another nearly linear structure, 2_0(b), depicted in Figure 1 with its B3LYP/6-31+G(d) level H···O···H angle of 177°, is obtained from the C_{2h} form by rotating one of the water molecules about the OO line, producing a local minimum with C_{2v} symmetry in the $^2B_1$ state. As with 2_0(a), the nearly linear local minimum found with B3LYP/6-31+G(d) disappears at higher levels of theory, becoming instead a transition state between two nonlinear local minima. As seen in Figure 3, with MP4(SDQ)/6-311+G(2d,p)//B3LYP/6-31+G(d) the lowest minimum lies at a H···O···H angle of 140°, and the other complementary minimum lying at 213° is only 0.03 kcal/mol higher, while the nearly linear transition state having a H···O···H angle of 178° lies 0.39 kcal/mol higher. This is again

a small barrier compared to the ZPVE, and we conclude that 2_0(b) can also be regarded as being nearly linear on average, but with many readily accessible bent conformations.

If the second water is introduced near the first water rather than near the O^-, the geometry optimization has quite a different outcome. A proton is transferred from the first water to the anion, resulting in a hydroxide anion to which a hydroxyl radical and a water molecule contribute hydrogen bonds in a 2^*_0 structure of the $(OH^-)(OH)(H_2O)$ form. This structure lies 0.6 kcal/mol higher in energy than the 2_0(a) global minimum. The 2_0* structure lacks the floppiness of 2_0(a) and 2_0(b).

Knak Jensen,[30] employing the MP2/6-31+G(d,p) method, and Seta et al.,[33] employing the B3LYP/aug-cc-pVDZ method, also report bent minima on the 2_0(a) and 2_0(b) potential surfaces, albeit at slightly different angles than our MP4(SDQ)/6-311+G-(2d,p)//B3LYP/6-31+G(d) results. For species of the $(OH^-)(OH)(H_2O)$ form, Knak Jensen finds a structure similar to our 2^*_0, which however is reported to lie 0.2 kcal/mol *below* his 2_0(a) C_s structure. This structure differs from the analogous one of Schindler et al.,[29] who used a pure DFT method with a polarized valence double-ζ basis set, in that the excess charge and the spin are localized on different OH groups, and the hydrogen bond from OH to OH^- is linear. Schindler et al. arrived at a minimum-energy configuration structure of the $(OH^-)(OH)(H_2O)$ form that would correspond to $1^*_1 1_0$ in our notation. When we tried to reproduce that structure using B3LYP/6-31+G(d), the optimization converged back to our previous C_s structure of 2_0-(a). However, when we substituted the pure DFT method BLYP for the hybrid B3LYP, we arrived at a minimum configuration which is qualitatively similar to that of Schindler et al., in which the excess charge and spin are distributed almost equally between the two OH moieties and the hydrogen bond that joined them is nonlinear. We conclude that the putative $1^*_1 1_0$ structure is spurious, being subject to the same failure for pure DFT observed in the $O_2H_2^-$ system.

The important point regarding $(O^-)(H_2O)_2$ structures of the 2_0 form, which has not previously been commented on, is that they are particularly difficult to characterize properly because of the shallowness and width of the potential basin in the H···O···H bending coordinate. A comparable phenomenon has been noted in the $F-(H_2O)_2$ system.[55] These 2_0 structures of $(O^-)(H_2O)_2$ can be regarded as being nearly linear on average, but quite fluxional regarding bending motions.

$O_4H_6^-$ Structures. We find five structures in the $(O^-)(H_2O)_3$ family, with four basic shapes as shown in Figure 1. The lowest-energy structure 3_0 is a planar C_{3h} pinwheel, essentially as reported by Bentley et al.,[32] having three hydrogen bonds to O^- but no water−water hydrogen bonds. A small distortion to provide one water−water hydrogen bond produces a 3_1 structure that lies 1.3 kcal/mol higher. A pair of $2_2 1_0$ ring structures, each having two hydrogen bonds to O^- and the third water molecule in a second solvation shell making two water−water hydrogen bonds, lie 3.0 and 3.2 kcal/mol above 3_0. A linear chain $2_1 1_0$ structure in which the second-shell water molecule forms only one water−water hydrogen bond lies at 4.1 kcal/mol. (One might expect $2_1 1_0$ to have a flat potential surface with respect to H···O···H bending about the oxygen anion. However, attempts to probe this behavior by varying the H···O···H angle, accompanied by constrained optimization of all other geometric parameters, resulted in structural rearrangement in the direction of the 3_1 and $2_2 1_0$ structures.) Note that in each of these $(O^-)(H_2O)_3$ structures the oxygen atoms together with those hydrogen atoms involved in making hydrogen bonds all lie nearly in a single plane, with the remaining dangling OH bonds generally pointing out of the plane.

We find six structures in the $(OH^-)(OH)(H_2O)_2$ family, with four basic shapes as shown in Figure 1. The lowest-energy structure 3^*_0 is nonplanar, having three hydrogen bonds to OH^- but no water−water hydrogen bonds, lying 1.8 kcal/mol above the lowest $(O^-)(H_2O)_3$ structure. A small distortion to provide one water−water hydrogen bond produces a 3^*_1 structure that lies only 0.1 kcal/mol higher than 3^*_0 (and lies significantly lower before making BSSE and ZPVE corrections). Four other structures, a pair of $2^*_2 1_0$ cases lying at 3.4 and 3.8 kcal/mol and a pair of $2^*_1 1_0$ cases lying at 4.8 kcal/mol, have two hydrogen bonds to OH^- and the third water molecule in a second solvation shell with hydrogen bonds either making a ring ($2^*_2 1_0$) or an open chain ($2^*_1 1_0$). Each of these latter four structures is topologically similar to an unstarred structure from the previous paragraph, but is about 0.5 kcal/mol less stable than its $(O^-)(H_2O)_3$ analogue.

The $2_2 1_0$ structure marks the first appearance of the square motif. This fragment is particularly stable because the water in the second solvent shell donates hydrogen bonds to both waters in the first shell, polarizing them and strengthening their hydrogen bonds to the anion. This unit reappears frequently in the structures of the four- and five-water clusters to be discussed below. The corresponding $2^*_1 1_0$ fragment is likewise stabilized.

Using the MP2/6-31+G(d,p) method, Knak Jensen[30] found five $O_4H_6^-$ structures, corresponding in our notation to 3^*_1, 3_0, 3_1, $2^*_2 1_0$(a), and $2_2 1_0$(a), as ordered by increasing electronic energy. Of particular note, the lowest-energy structure 3^*_1 he reported has the $(OH^-)(OH)(H_2O)_2$ form, with the 3_0 structure having the $(O^-)(H_2O)_3$ form lying 1.1 kcal/mol higher; we instead find these to be in the opposite order. Using a pure DFT method, Schindler et al.[29] found two $2^*_1 1_0$ structures and the 3_0 structure, which were described as being roughly equal in energy, a conclusion which is now clearly incorrect. Their $2^*_1 1_0$ differs from ours in being an open structure; our attempts to reproduce it resulted in ring closure leading back to our $2^*_2 1_0$ structure.[56] Using the B3LYP/aug-cc-pVDZ method including ZPVE, Seta et al.[33] reported the 3_0 and 3^*_0 structures, with the latter 1.8 kcal/mol above the former, in good agreement with our results.

$O_5H_8^-$ Structures. We have identified twelve structures in the $(O^-)(H_2O)_4$ family, with eight basic shapes as illustrated in Figure 4. The lowest in energy are a pair of 4_2 structures each having two water molecules forming a nearly planar hydrogen bonded ring on each side of the O^-. Slightly higher (and in fact lower before making BSSE corrections) is a pair of $3_2 1_0$ structures that are derived from the $2_2 1_0$ structures of $O_4H_6^-$ by adding a fourth water which makes a hydrogen bond to the O^-. About 2 kcal/mol above the 4_2(a) global minimum are three $3_2 1_0$ structures (cases c, d, and e) which derive from 3_1 by adding a water in the second solvation shell. Of comparable energy is a $3_1 1_1$ structure resembling $3_2 1_0$(a or b) but with a rearranged hydrogen bonding scheme. About 1 kcal/mol higher in energy than this group are the 4_4 and $3_2 1_1$(a and b) structures. The former is a complex of C_4 symmetry in which each water donates a hydrogen bond to O^- and to an adjacent water. The latter are trigonal bipyramids with O^- at an apex. These arise from adding a fourth water to the 3_0 structure in such a way that it forms three new hydrogen bonds. In each of these systems, the arrangement of hydrogen bonds around O^- places the anion at the apex of a pyramid. If two hydrogen bonds were to be broken in 4_4, it would relax to 4_2(a). Likewise, if only one hydrogen bond were to be broken in the $3_2 1_1$ structures,

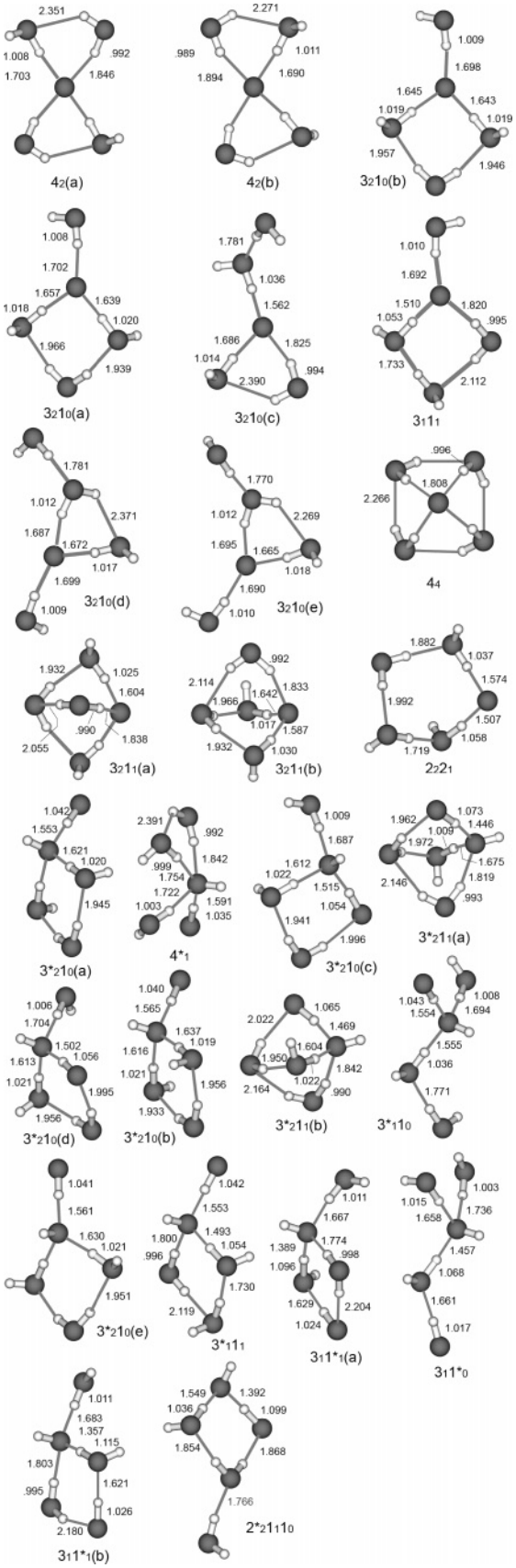

Figure 4. B3LYP/6-31+G(d) structures of $O_5H_8^-$ clusters.

they would relax to 3_21_0(a) or 3_11_1. It appears that the energy gained by forming additional hydrogen bonds is more than canceled by that needed to distort the system from planarity. Finally, 5.8 kcal/mol above the lowest structure is a 2_22_1 structure in which the oxygen nuclei describe a five-membered ring. It is possible that there exist stable structures in which the hydrogen bond network is an open chain, but they will undoubtedly lie still higher in energy, and we did not search for them.

The fourteen structures in the $(OH^-)(OH)(H_2O)_3$ family have five basic forms, if we regard OH and H_2O as interchangeable units, or eleven otherwise (see Figure 4). Lowest in energy is $3^*_21_0$(a), 0.8 kcal/mol above 4_2(a) and 0.5 kcal/mol above its O^- analogue, 3_21_0(a). The 4^*_1 structure is 1.5 kcal/mol above 4_2(a). Only slightly higher in energy are the other $3^*_21_0$ structures and the $3^*_21_1$ trigonal bipyramids. Lying more than 3 kcal/mol above the global minimum 4_2(a) structure are the open $3^*_11_0$ and $3_11^*_0$ structures and the $2^*_21_11_0$ structure, in which a third solvation shell is populated. In general, energies of $(OH^-)(OH)(H_2O)_3$ structures lie from 0.7 to 1.3 kcal/mol above those of the analogous $(O^-)(H_2O)_4$ structures. The $3^*_21_1$ trigonal bipyramids constitute a notable exception: they lie 1.5 kcal/mol *below* the corresponding 3_21_1 structures. The reason for this is clear. The hydrogen bonding pattern around the hydroxide oxygen is preferentially nonplanar, so the fourth water need not distort the existing hydrogen bond network as happens with the 3_21_1 systems.

The 8 structures of $O_5H_8^-$ reported by Knak Jensen[30] from MP2/6-31+G(d,p) calculations are among the 26 structures described here and include the lowest-energy structure for each anion type. His energetic trends are similar to ours within each family, but he consistently finds the oxygen anion clusters shifted to higher energies by about 2 kcal/mol relative to the hydroxide clusters. Seta et al.[33] reported only a 4_0 structure, being nonplanar with a distorted rectangular shape, and the corresponding 4^*_0 structure, which they find 1.4 kcal/mol higher in energy, consistent with our results for 4_2 and 4^*_1.

$O_6H_{10}^-$ Structures. We have identified eleven structures in the $(O^-)(H_2O)_5$ family, with ten basic shapes as illustrated in Figure 5. The lowest in energy is a 4_31_0 structure in which O^- is part of a three-oxygen ring and a separate four-oxygen ring. Nearby in energy are a 3_42_0 structure best described as two fused squares (the "book" form, +0.8 kcal/mol), a 4_41_1 structure related to 4_31_0(a) by distorting it to form two additional hydrogen bonds (+1.1 kcal/mol), and a $3_21_11_0$ structure obtained from 3_21_0(a) by adding a fifth water which makes a hydrogen bond to the second-shell water (+1.5 kcal/mol). All of these structures arise from adding a fifth water to the 3_21_0 structures of the previous section and, except for 4_41_1, tend to maintain planarity about O^-. About 2 kcal/mol above 4_31_0(a) are 4_31_0(b), which arises from starting a second solvent shell around 4_2(a), 5_5, which is approximately C_5 in symmetry, and 3_22_1, which derives from 2_22_1 by adding a fifth water that makes a hydrogen bond directly to O^-. Still higher are a second 4_41_1 structure, a pair of 3_32_2 structures that resemble the $(H_2O)_6$ prism structure with one hydrogen bond broken, and a $2_22_31_0$ structure with only two hydrogen bonds to O^-. Aside from the last, these higher-energy structures all have nonplanar arrangements of hydrogen bonds about O^-.

Among the fifteen structures found in the $(OH^-)(OH)(H_2O)_4$ family (see Figure 5), the lowest-energy structure is the prismlike $3^*_32_2$(a), which lies 1.1 kcal/mol above the global minimum 4_31_0(a) form. Slightly higher (at 1.6 and 1.7 kcal/mol, respectively) are $3_32^*_0$ and a second prism, $3^*_32_2$(c). Lying between 2 and 3 kcal/mol above 4_31_0(a) are six structures encompassing a wide array of forms: squares, squares with fused triangles, books, and a cagelike structure. An even larger group lies 4.5 kcal/mol and higher above the minimum; see Table 1 and Figure

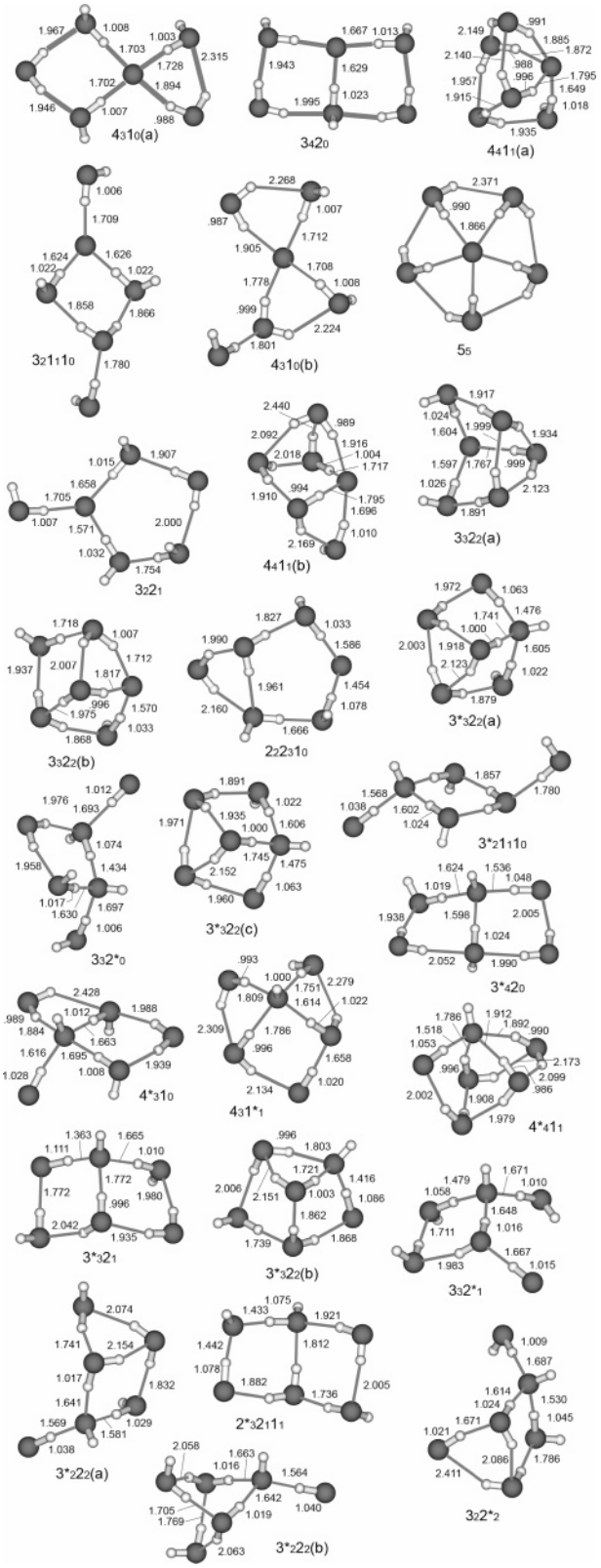

Figure 5. B3LYP/6-31+G(d) structures of $O_6H_{10}^-$ clusters.

5 for details. What these high-lying forms have in common is twofold coordination of the hydroxide anion or geometric constraints that weaken some of the hydrogen bonds.

At the $O_6H_{10}^-$ stage, it is more difficult to find direct analogues between members of the $(O^-)(H_2O)_5$ family and those of the $(OH^-)(OH)(H_2O)_4$ family. Where such relationships can be discerned, the O^- structure is typically at least 1 kcal/mol more stable than the corresponding OH^- structure. The exceptions are the $3^*{}_32_2$ prism structures, which are about 2 kcal/mol more stable than their O^- analogues. Once again, the reason is that the nonplanar hydrogen bonding arrangement about the anion destabilizes $(O^-)(H_2O)_5$ complexes but not $(OH^-)(OH)(H_2O)_4$ complexes.

Knak Jensen[30] using UHF/6-31+G(d,p) methods described six structures of $O_6H_{10}^-$, which correspond most closely to our structures 4_31_0, 4_41_1, 3_42_0, $4^*{}_31_0$, $3^*{}_32_2$(a), and $3^*{}_22_2$. His energetic trends are generally within 1 kcal/mol of ours, but his E_5 structure is 2.4 kcal/mol above his lowest-energy structure, whereas our corresponding $3^*{}_32_2$(a) structure is only 1.1 kcal/mol above our lowest-energy structure. The trend observed for smaller clusters, that Knak Jensen finds greater stabilization of the hydroxide clusters relative to the oxygen anion clusters than we do, is not reproduced for $O_6H_{10}^-$. A possible explanation is that his $O_6H_{10}^-$ results were obtained with Hartree−Fock methods, whereas all his results for smaller clusters arise from MP2 methods.

Hydrogen Bonding Patterns. At all cluster sizes considered here, oxygen anion clusters are energetically favored over hydroxide clusters, on the basis of the most stable structure of each type. The number of structures of each type increases rapidly with n, and for $n \geq 3$, the energies of the two families overlap. In the $(O^-)(H_2O)_n$ families, there is an energetic advantage if the hydrogen bonds to the oxygen anion lie in a plane, and clusters which accommodate this pattern are generally lower in energy than those which distort the plane to form additional hydrogen bonds among the solvating waters. This is the case whether the oxygen anion is triply or quadruply coordinated. In $(OH^-)(OH)(H_2O)_{n-1}$ clusters, on the other hand, the preference is for the first solvation shell not to lie in a plane. The hydroxide oxygen behaves as if it were maintaining sp^3 hybridization. This qualitative difference is due to the radical nature of O^-. The 2p hole on O^- defines an axis of relative electron depletion, which is not electrostatically conducive to the formation of hydrogen bonds. A consequence of this is that the O^- is always on the surface of any cluster it is in, with its unpaired electron not involved in hydrogen bonding but directed normal to the surface and thus accessible to potential reactants.

It is clear from the data shown in Figures 1, 4, and 5 that in all $(O^-)(H_2O)_n$ clusters those water OH bonds which are directly hydrogen bonded to the O^- moiety are always significantly stretched from that of the isolated water molecule, in which it is 0.969 Å at the B3LYP/6-31+G(d) level. Such stretchings range from 0.098 Å for $n = 1$, from 0.058 to 0.063 Å for $n = 2$, from 0.031 to 0.090 Å for $n = 3$, from 0.02 to 0.089 Å for $n = 4$, and from 0.018 to 0.109 Å for $n = 5$. It is interesting that the largest such stretching of 0.109 Å is in $2_22_31_0$, which is the least stable form of $(O^-)(H_2O)_5$ found, while the other notably large stretching of 0.098 Å is in the 1_0 structure of $(O^-)(H_2O)$.

It is also clear from Figures 1, 4, and 5 that in all $(OH^-)(OH)(H_2O)_{n-1}$ clusters both water and hydroxyl OH bonds which are directly hydrogen bonded to the OH^- moiety are also always significantly stretched from that in the respective isolated molecule, in which it is 0.983 Å for the hydroxyl radical at the B3LYP/6-31+G(d) level. Such stretchings for water OH bonds range from 0.058 Å for $n = 2$, from 0.031 to 0.104 Å for $n = 3$, from 0.021 to 0.146 Å for $n = 4$, and from 0.017 to 0.105 Å for $n = 5$. The stretchings are even larger on average for hydroxyl OH bonds, which range from 0.087 Å for $n = 2$, from 0.068 to 0.107 Å for $n = 3$, from 0.052 to 0.116 Å for $n = 4$, and from 0.045 to 0.128 Å for $n = 5$.

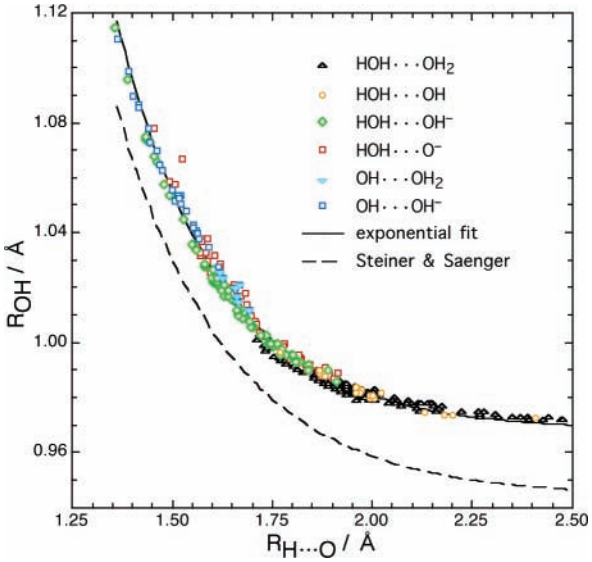

Figure 6. Covalent OH bond lengths for all 335 of the H···O hydrogen bonds contained in the 67 minimum energy B3LYP/6-31+G(d) structures of $O_{n+1}H_{2n}^-$ obtained in this work.

Although we do not pursue the matter here, it can also be noted that there is significant anharmonicity in the stretching vibrational motions of all such OH bonds having stretched equilibrium values.

It has long been recognized in the experimental diffraction literature[57] that there is an inverse correlation between the length of an OH covalent bond (R_{OH}) and that of the H···O hydrogen bond ($R_{H\cdots O}$) in which it is involved. The 67 minimum-energy structures of Table 1 provide a database of 335 hydrogen bonds of the form OH···O (defining a hydrogen bond as any H···O interaction having distance < 2.5 Å) that can be used to test such a correlation. These bond lengths are plotted against each other in Figure 6. Six types of interaction occur here: H_2O can serve as a hydrogen bond donor to another H_2O, to OH, to O^-, or to OH^-; and OH can serve as a donor to H_2O or to OH^-. Hydrogen bonds involving anions fall preferentially on the left side of the graph, and those involving only neutral species are toward the right. Nevertheless, all forms lie near the same curve with rather little dispersion. The smallest possible cluster, $(O^-)(H_2O)$, is also the only point which lies any appreciable distance off the curve. There is a general connection between the length of the hydrogen bond and its strength, but the stability of a particular cluster cannot be inferred from the data in Figure 6. Energetics are established by competition and cooperation between the various possible hydrogen bonds, but once this equilibrium is achieved, all the hydrogen bonds are found to obey the general relationship of Figure 6.

One can further subdivide the cases according to the donor's participation in the hydrogen bonding network: d for a molecule that only donates, dd for one that donates two hydrogen bonds, da for one that both donates and accepts, and dda or daa for those that participate in three hydrogen bonds. (The present database affords no examples of ddaa, the final possibility.) In general, these cases cluster on the curve of Figure 6 in the following order, from left to right: daa, da, dda, d, dd.

Steiner and Saenger[58] examined bond lengths in OH···O systems derived from low-temperature neutron diffraction data for a wide variety of crystals including carbohydrates, organic acids, phosphates, carboxylates, and water of hydration and fitted the results using an exponential function: $R_{OH} = R_{OH}^\circ + A \exp(-\beta R_{H\cdots O})$. Applying the same function, we obtain the solid line in Figure 6 that is an excellent fit to our B3LYP/6-31+G-(d) data. This fit also compares reasonably well with the dashed line that represents the analogous fit to experimental data by Steiner and Saenger[59] except for a systematic offset of 0.026 ± 0.005 Å in the OH bond length. Clearly, this length correlation in the hydrogen bonding subsystem is hardly affected by the molecular environment from which it is taken.

Implications for Cluster Formation. The energetic stabilization due to each additional water molecule, based on the lowest-energy structure of each size, is 24 kcal/mol for the first water, 17 for the second, 14 for the third, 10 for the fourth, and 9 for the fifth. The stabilization energies of the clusters are determined more by the number of water molecules than by the number of hydrogen bonds. For instance, in the case of $O_6H_{10}^-$, the number of hydrogen bonds in the various structures ranges between 6 and 10, but the 26 reported structures all lie within 7.3 kcal/mol of one another.

This closeness in energies of analogous $(O^-)(H_2O)_n$ and $(OH^-)(OH)(H_2O)_{n-1}$ clusters suggests that interconversion should be facile. That is undoubtedly the case in aqueous media, and in several geometry optimization runs we observed such interconversions to occur by proton migration within a hydrogen bond. In all such instances, the initial configuration involved an anion with few coordinating hydrogen bonds, and in the final configuration, a nearby more highly coordinated water or hydroxyl had transferred its proton to the original anion. However, there are in Table 1 no two clusters that are related to each other by a simple proton transfer across a hydrogen bond. In every case, the proton transfer must be accompanied by a breaking and reformation of the hydrogen bond network for interconversion to proceed. Thus, while the present results emphasize the variety and complexity of the $O_{n+1}H_{2n}^-$ potential surfaces, without extensive further studies of the interconversion barriers very little can be said directly about dynamics on those surfaces. We can, however, use the reported structures and our experience with geometry optimizations to make some preliminary inferences about the process of cluster formation in the gas phase.

If a cluster forms by sequential addition of water molecules to an oxygen anion, its type is likely to be determined by the second or third addition. If the second water approaches in a way that promotes a hydrogen bond to the anionic center, proton transfer is unlikely. If, however, the second water approaches in a way that promotes hydrogen bonding to the first water, then proton transfer will probably occur. The same likelihoods apply to the addition of the third water, except that if the third water forms two donor hydrogen bonds to the other waters the structure will remain an oxygen anion structure. As additional waters are added, the anion of either type is stabilized well enough by its first three waters that proton transfer becomes unlikely.

If anion clusters are formed by reaction of a bare O^- with a water cluster, the ultimate type depends on how many hydrogen bonds can be formed to the O^- with minimal disruption of the existing hydrogen bond network. In this situation, initial formation of a single hydrogen bond to O^- will very likely result in proton transfer. For initial formation of two hydrogen bonds to O^-, the outcome will depend on how well-coordinated the neighboring waters are. Initial formation of three or more hydrogen bonds to O^- will not result in proton transfer.

If large clusters form by the interaction of smaller clusters, there are too many possibilities to make a general prediction, but the guiding principle in examining specific cases is that proton transfer will probably take place to favor that form of the anion which is more highly coordinated by hydrogen bonds.

It is also possible for $(O^-)(H_2O)_n$ and $(OH^-)(OH)(H_2O)_{n-1}$ clusters to interconvert by means of hydrogen atom transfers. Klaning et al.[7] used oxygen isotopic labeling to determine that in irradiated aqueous solution hundreds of reversible proton transfers between H_2O and O^- take place for each hydrogen atom transfer, with the net result that overall about 78% of successful reaction events occur by transfer of a proton and the remaining 22% by hydrogen atom transfer. We saw no evidence of hydrogen atom transfer in our studies, although that means little since the methods we employed may be unreliable for exploration of hydrogen atom transfer pathways.

Conclusion

In the monohydrate $O_2H_2^-$, very high level QCISD(T)/aug-cc-pVTZ//QCISD/aug-cc-pVTZ calculations confirm that the most stable structure is the planar 1_0 form $(O^-)(H_2O)$. A proton-transferred moiety 1^*_0 of $(OH^-)(OH)$ form lies significantly higher (~2 kcal/mol) on the potential surface and is not a local minimum. For this system, the more efficient MP4(SDQ)/6-311+G(2d,p)//B3LYP/6-31+G(d) and MP4(SDQ)/6-311+G-(2d,p) methods give results very close to those of the presumably accurate QCISD(T)/aug-cc-pVTZ//QCISD/aug-cc-pVTZ method, whereas MP2 methods fail qualitatively and in different ways depending on the basis set chosen. On the basis of these findings, the MP4(SDQ)/6-311+G(2d,p)//B3LYP/6-31+G(d) method is used here to obtain most results on the larger clusters.

In $O_3H_4^-$, the most stable structure is the planar fluxional 2_0(a) form of $(O^-)(H_2O)_2$. The electronic potential energy surface along the H···O···H bending coordinate is very flat, such that ZPVE allows for large-amplitude motion between two equivalent bent minima connected by a linear transition state. In $O_4H_6^-$, $O_5H_8^-$, and $O_6H_{10}^-$, the most stable structures are again of the $(O^-)(H_2O)_n$ form. With $n \geq 3$, the various $(O^-)(H_2O)_n$ structures "lock in", and large-amplitude bending motions are not of concern, nor are they of consequence for any of the $(OH^-)(OH)(H_2O)_{n-1}$ structures.

For $n \geq 2$, a number of higher-energy structures of both the $(O^-)(H_2O)_n$ and $(OH^-)(OH)(H_2O)_{n-1}$ forms exist with interleaving energies and a variety of interesting geometrical motifs. The lower-energy $(O^-)(H_2O)_n$ structures tend to have planar or nearly planar coordination of first-shell hydrogen bonds about a central O^- such that the unpaired electron lies in a p-like orbital on oxygen directed perpendicular to the plane and not involved in a hydrogen bond. The various $(OH^-)(OH)(H_2O)_{n-1}$ structures, on the other hand, usually have nonplanar coordination of first-shell hydrogen bonds about the anionic center.

No cases are found of OH^- acting as a hydrogen bond donor.

The BSSE correction decreases the binding energy of each complex. It has a further differential effect in destabilizing $(OH^-)(OH)(H_2O)_{n-1}$ structures by at least 1.1 kcal/mol relative to analogous $O^-(H_2O)_n$ structures. It also leads to some changes in the order of stability within the separate $O^-(H_2O)_n$ and $(OH^-)(OH)(H_2O)_{n-1}$ families, generally benefiting those structures with relatively fewer hydrogen bonds between water molecules.

The inclusion of ΔZPVE also decreases the binding energy of each complex. It generally stabilizes $(OH^-)(OH)(H_2O)_{n-1}$ relative to analogous $O^-(H_2O)_n$ structures, although this effect is somewhat less than the BSSE correction that acts in the opposite direction. It also sometimes has a substantial effect on the binding energy ordering, generally benefiting those structures with the lowest total number of hydrogen bonds.

In all structures, the first-shell water or hydroxyl OH bonds that hydrogen bond to an anionic center are significantly stretched by amounts ranging 0.017−0.146 Å from their equilibrium value in the respective isolated molecule, with hydroxyl OH bonds being stretched on average more than water OH bonds. This is accompanied by significant anharmonicity in the OH stretching vibrational motions of all such stretched OH bonds.

For all the hydrogen bonds in the clusters examined in this work, a quantitative inverse correlation is found between the length of an OH covalent bond and that of the H···O hydrogen bond in which it is involved. Expressing this correlation with a functional form taken from the literature[58] produces an excellent fit to our data which also agrees well, except for a systematic offset, with the fit obtained experimentally from neutron diffraction measurements on a wide variety of hydrogen bonds.

In the formation of clusters from components, and in the interconversion of $(O^-)(H_2O)_n$ and $(OH^-)(OH)(H_2O)_{n-1}$, our general observation is that the most stable of several possible forms involves the greatest coordination of the anion by hydrogen bonds.

Finally, it should be mentioned that the lower-energy structures found in this work are likely candidates for carriers of the infrared vibrational spectra recently observed[34] experimentally for $O_{n+1}H_{2n}^-$ clusters having $n = 1-5$. The most likely candidates can be subjected to further refinement of their structures and determination of their force fields to aid the interpretation of these experiments.

Acknowledgment. The research described here was supported by the Office of Basic Energy Science of the U. S. Department of Energy. This is contribution no. NDRL-4603 from the Notre Dame Radiation Laboratory.

Supporting Information Available: Cartesian coordinates and unscaled harmonic vibrational frequencies for the B3LYP/6-31+G(d) local-minimum structures found in this work. This material is available free of charge via the Internet at http://pubs.acs.org.

References and Notes

(1) Spinks, J. W. T.; Woods, R. J. *An Introduction to Radiation Chemistry*, 3rd ed.; Wiley: New York, 1990.
(2) Hickel, B.; Corfitzen, H.; Sehested, K. *J. Phys. Chem.* **1996**, *100*, 17186.
(3) Poskrebyshev, G. A.; Neta, P.; Huie, R. E. *J. Phys. Chem. A* **2002**, *106*, 11488.
(4) Czapski, G. Radiation Chemistry of Oxygenated Aqueous Solutions. In *Annual Review of Physical Chemistry*; Eyring, H., Christensen, C. J., Johnston, H. S., Eds.; Kingsport Press: Palo Alto, 1971; Vol. 22, p 171.
(5) Buxton, G. V.; Greenstock, C. L.; Helman, W. P.; Ross, A. B. *J. Phys. Chem. Ref. Data* **1988**, *17*, 513.
(6) Lee, J.; Grabowski, J. J. *Chem. Rev.* **1992**, *92*, 1611.
(7) Klaning, U. K.; Larsen, E.; Sehested, K. *J. Phys. Chem.* **1994**, *98*, 8946.
(8) Symons, M. C. R. *J. Chem. Soc., Faraday Trans. 1* **1982**, *78*, 1953.
(9) Knewstubb, P. F.; Sugden, T. M. *Nature (London)* **1962**, *196*, 1311.
(10) Melton, C. E. *J. Phys. Chem.* **1972**, *76*, 3116.
(11) Fehsenfeld, F. C.; Ferguson, E. E. *J. Chem. Phys.* **1974**, *61*, 3181.
(12) Lifshitz, C. *J. Phys. Chem.* **1982**, *86*, 3634.
(13) Van Doren, J. M.; Barlow, S. E.; DePuy, C. H.; Bierbaum, V. M. *Int. J. Mass Spectrom.* **1991**, *109*, 305.
(14) Varley, D. F.; Levandier, D. J.; Farrar, J. M. *J. Chem. Phys.* **1992**, *96*, 8806.
(15) Buntine, M. A.; Lavrich, D. J.; Dessent, C. E.; Scarton, M. G.; Johnson, M. A. *Chem. Phys. Lett.* **1993**, *216*, 471.
(16) Arnold, D. W.; Xu, C. S.; Neumark, D. M. *J. Chem. Phys.* **1995**, *102*, 6088.
(17) Deyerl, H. J.; Clements, T. G.; Luong, A. K.; Continetti, R. E. *J. Chem. Phys.* **2001**, *115*, 6931.
(18) Yang, X.; Castleman, A. W. *J. Phys. Chem.* **1990**, *94*, 8500.
(19) Pataki, L.; Mady, A.; Venter, R. D.; Poirier, R. A.; Peterson, M. R.; Csizmadia, I. G. *THEOCHEM* **1986**, *135*, 189.

(20) Tang, T. H.; Csizmadia, I. G.; Pataki, L.; Venter, R. D.; Ward, C. A. *THEOCHEM* **1991**, *233*, 185.
(21) Tang, T. H.; Csizmadia, I. G.; Pataki, L.; Venter, R. D.; Ward, C. A. *THEOCHEM* **1992**, *276*, 97.
(22) Viggiano, A. A.; Morris, R. A.; Deakyne, C. A.; Dale, F.; Paulson, J. F. *J. Phys. Chem.* **1990**, *94*, 8193.
(23) Roehl, C. M.; Snodgrass, J. T.; Deakyne, C. A.; Bowers, M. T. *J. Chem. Phys.* **1991**, *94*, 6546.
(24) Benassi, R.; Taddei, F. *Chem. Phys. Lett.* **1993**, *204*, 595.
(25) Humbel, S.; Demachy, I.; Hiberty, P. C. *Chem. Phys. Lett.* **1995**, *247*, 126.
(26) Knak Jensen, S. J.; Klaning, U. K. *Chem. Phys. Lett.* **1995**, *241*, 404.
(27) Hrusak, J.; Friedrichs, H.; Schwarz, H.; Razafinjanahary, H.; Chermette, H. *J. Phys. Chem.* **1996**, *100*, 100.
(28) Knak Jensen, S. J.; Csizmadia, I. G. *THEOCHEM* **1998**, *455*, 69.
(29) Schindler, T.; Berg, C.; Niedner-Schatteburg, G.; Bondybey, V. E. *J. Phys. Chem.* **1995**, *99*, 12434.
(30) Knak Jensen, S. J. *THEOCHEM* **2000**, *498*, 69.
(31) Knak Jensen, S. J. *THEOCHEM* **2002**, *578*, 63.
(32) Bentley, J.; Collins, J. Y.; Chipman, D. M. *J. Phys. Chem. A* **2000**, *104*, 4629, 4670.
(33) Seta, T.; Yamamoto, M.; Nishioka, M.; Sadakata, M. *J. Phys. Chem. A* **2003**, *107*, 962.
(34) Johnson, M. A. Personal communication.
(35) Becke, A. D. *J. Chem. Phys.* **1993**, *98*, 5648.
(36) Lee, C. T.; Yang, W. T.; Parr, R. G. *Phys. Rev. B* **1988**, *37*, 785.
(37) Ditchfield, R.; Hehre, W. J.; Pople, J. A. *J. Chem. Phys.* **1971**, *54*, 724.
(38) Hariharan, P. C.; Pople, J. A. *Theor. Chim. Act.* **1973**, *28*, 213.
(39) Clark, T.; Chandrasekhar, J.; Spitznagel, G. W.; Schleyer, P. V. *J. Comput. Chem.* **1983**, *4*, 294.
(40) Scott, A. P.; Radom, L. *J. Phys. Chem.* **1996**, *100*, 16502.
(41) Moller, C.; Plesset, M. S. *Phys. Rev.* **1934**, *46*, 618.
(42) Krishnan, R.; Pople, J. A. *Int. J. Quantum Chem.* **1978**, *14*, 91.
(43) Krishnan, R.; Binkley, J. S.; Seeger, R.; Pople, J. A. *J. Chem. Phys.* **1980**, *72*, 650.
(44) Frisch, M. J.; Pople, J. A.; Binkley, J. S. *J. Chem. Phys.* **1984**, *80*, 3265.
(45) Boys, S. F.; Bernardi, F. *Mol. Phys.* **1970**, *19*, 553.
(46) Pople, J. A.; Head-Gordon, M.; Raghavachari, K. *J. Chem. Phys.* **1987**, *87*, 5968.
(47) Dunning, T. H. *J. Chem. Phys.* **1989**, *90*, 1007.
(48) Kendall, R. A.; Dunning, T. H.; Harrison, R. J. *J. Chem. Phys.* **1992**, *96*, 6796.
(49) Frisch, M. J.; Trucks, G. W.; Schlegel, H. B.; Scuseria, G. E.; Robb, M. A.; Cheeseman, J. R.; Zakrzewski, V. G.; Montgomery, J. A., Jr.; Stratmann, R. E.; Burant, J. C.; Dapprich, S.; Millam, J. M.; Daniels, A. D.; Kudin, K. N.; Strain, M. C.; Farkas, O.; Tomasi, J.; Barone, V.; Cossi, M.; Cammi, R.; Mennucci, B.; Pomelli, C.; Adamo, C.; Clifford, S.; Ochterski, J.; Petersson, G. A.; Ayala, P. Y.; Cui, Q.; Morokuma, K.; Malick, D. K.; Rabuck, A. D.; Raghavachari, K.; Foresman, J. B.; Cioslowski, J.; Ortiz, J. V.; Stefanov, B. B.; Liu, G.; Liashenko, A.; Piskorz, P.; Komaromi, I.; Gomperts, R.; Martin, R. L.; Fox, D. J.; Keith, T.; Al-Laham, M. A.; Peng, C. Y.; Nanayakkara, A.; Gonzalez, C.; Challacombe, M.; Gill, P. M. W.; Johnson, B. G.; Chen, W.; Wong, M. W.; Andres, J. L.; Head-Gordon, M.; Replogle, E. S.; Pople, J. A. *Gaussian 98*, revision A.11; Gaussian, Inc.: Pittsburgh, PA, 1998.
(50) Frisch, M. J.; Trucks, G. W.; Schlegel, H. B.; Scuseria, G. E.; Robb, M. A.; Cheeseman, J. R.; Montgomery, Jr., J. A.; Vreven, T.; Kudin, K. N.; Burant, J. C.; Millam, J. M.; Iyengar, S. S.; Tomasi, J.; Barone, V.; Mennucci, B.; Cossi, M.; Scalmani, G.; Rega, N.; Petersson, G. A.; Nakatsuji, H.; Hada, M.; Ehara, M.; Toyota, K.; Fukuda, R.; Hasegawa, J.; Ishida, M.; Nakajima, T.; Honda, Y.; Kitao, O.; Nakai, H.; Klene, M.; Li, X.; Knox, J. E.; Hratchian, H. P.; Cross, J. B.; Bakken, V.; Adamo, C.; Jaramillo, J.; Gomperts, R.; Stratmann, R. E.; Yazyev, O.; Austin, A. J.; Cammi, R.; Pomelli, C.; Ochterski, J. W.; Ayala, P. Y.; Morokuma, K.; Voth, G. A.; Salvador, P.; Dannenberg, J. J.; Zakrzewski, V. G.; Dapprich, S.; Daniels, A. D.; Strain, M. C.; Farkas, O.; Malick, D. K.; Rabuck, A. D.; Raghavachari, K.; Foresman, J. B.; Ortiz, J. V.; Cui, Q.; Baboul, A. G.; Clifford, S.; Cioslowski, J.; Stefanov, B. B.; Liu, G.; Liashenko, A.; Piskorz, P.; Komaromi, I.; Martin, R. L.; Fox, D. J.; Keith, T.; Al-Laham, M. A.; Peng, C. Y.; Nanayakkara, A.; Challacombe, M.; Gill, P. M. W.; Johnson, B.; Chen, W.; Wong, M. W.; Gonzalez, C.; Pople, J. A. *Gaussian 03*, Revision C.01; Gaussian, Inc., Wallingford CT, 2004.
(51) Xantheas, S. S. *J. Am. Chem. Soc.* **1995**, *117*, 10373.
(52) Masamura, M. *J. Chem. Phys.* **2002**, *117*, 5257.
(53) Maheshwary, S.; Patel, N.; Sathyamurthy, N.; Kulkarni, A. D.; Gadre, S. R. *J. Phys. Chem. A* **2001**, *105*, 10525.
(54) The harmonic frequency for the normal mode corresponding to H···O···H bending therefore has little real relevance, but even so, we do not attempt to make any explicit correction to the total energy for the anharmonicity, because the zero-point harmonic vibrational energy in this mode is only 0.035 kcal/mol.
(55) Ayotte, P.; Nielsen, S. B.; Weddle, G. H.; Johnson, M. A.; Xantheas, S. S. *J. Phys. Chem. A* **1999**, *103*, 10665.
(56) Whether this optimization arrives at 2_21_0(a) or 2_21_0(b) depends on the relative orientation of the dangling OH bonds in the starting structure, a parameter not specified by Schindler et al.
(57) Nakamoto, K.; Margoshes, M.; Rundle, R. E. *J. Am. Chem. Soc.* **1955**, *77*, 6480.
(58) Steiner, T.; Saenger, W. *Acta Crystallogr., Sect. B* **1994**, *50*, 348.
(59) Fitting to our B3LYP/6-31+G(d) data gives $R_{OH}^{\circ} = 0.968$ Å, $A = 28.9$ Å, and $\beta = 3.87$ Å^{-1}, compared to the respective parameters of 0.944 Å, 17.7 Å, and 3.55 Å^{-1} found in the fit to experimental data by Steiner and Saenger.